CLAS-NOTE 98-014

NEUTRON DETECTION IN THE CLAS CALORIMETERS A FIRST MEASUREMENT

Erin Hackett
Roanoke College
UPR Program
Thomas Jefferson National Accelerator Facility
August 5, 1998

mentor: Will Brooks

NEUTRON DETECTION IN THE CLAS CALORIMETERS A FIRST MEASUREMENT

Erin Hackett
Roanoke College
Thomas Jefferson National Accelerator Facility
UPR Program

August 5, 1998

Abstract

The reaction ep->e'nπ^+ was explored to determine the ability of CLAS to detect neutrons. The bulk of the study was determining the neutron detection efficiency of the calorimeters in CLAS. Several cuts were made to unambiguously identify these final state particles. An efficiency plot was then created as a function of neutron momentum. In addition to this the angular resolution for neutrons was examined. Also, the manner in which neutrons deposit their energy was briefly explored. An attempt to separate photons and neutrons was made unsuccessfully and the reasons for its failures are also reported.

August 5, 1998

Neutron Detection in the CLAS Calorimeters- A First Measurement

Erin Hackett

Jefferson Lab (UPR program)

Introduction

JEFFERSON LAB

The Continuous Electron Beam Accelerator, located at Jefferson Lab in Newport News, Virginia, is a new facility where scientists perform research on atomic nuclei. The accelerator is shaped like a racetrack, and runs in underground tunnels which are almost a mile around. The beam consists of high energy electrons, which can have up to 4 GeV of energy. After the beam circuits around the accelerator to reach its desired energy, it is then channeled into the three experimental research halls at the lab. The research halls contain various detectors, each of which specialize in different types of experiments and aspects of detection.

HALL B

Hall B specializes in the detection of multi-particle final states through the use of the CEBAF Large Acceptance Spectrometer (CLAS). From the outside, CLAS appears like a sphere, and in the center of that sphere is the target for the electron (or photon) beam. Therefore, when the beam strikes the target a very high percentage of the particles produced by the scattering can be detected by the detector. This sphere is actually made up of layers of different detectors, each doing something different to help reconstruct and identify the final state particles. In contrast to the other halls, Hall B does not have extremely good resolution in its detectors, but it is the only hall that can detect such a wide range of angles, momenta, and number of particles. Inside the CLAS, a toroidal magnetic field is produced by six (iron-free) superconducting coils. There are also drift chambers which determine the charged particles' trajectories. In addition to this, there are scintillation counters which provide the researcher with time-of-flight data, as well

as Cerenkov counters that identify electrons. On the very outside of the CLAS in the forward direction are six electromagnetic shower calorimeters which also detect a variety of particles.

FORWARD CALORIMETER

Each calorimeter is triangular shaped, and the six of them fit together on the exterior of the CLAS. A calorimeter consists of scintillator strips that run parallel to the three axes of the triangle (axes U, V, and W). When the calorimeter is hit, light is produced in these three axes. The light travels to a photomultiplier tube which produces an electric pulse. This pulse is sent through an analog-to-digital converter, and this digital readout is what is recorded. Neutrons are detected by their hadronic interaction in the lead or scintillation material of the calorimeter leading to charged particles in the final state. This detector is able to identify electrons and separate them from pions as well as distinguish between photons and neutrons. This detector is predicted to have a good neutron detection efficiency, at least 50 percent.

EXPERIMENT RELEVANCE

An important parameter in the analysis of experimental data is the accuracy of the detector. For a researcher doing an experiment using the data the detector provided on neutrons, it is obviously important to recognize the limitations of the detector in addition to its capabilities. It was stated above that the calorimeter is predicted to have a good neutron detection efficiency, however exactly how efficient it is has not yet been explored at Jefferson Lab. This knowledge would be very beneficial to many researchers who will be doing research involving neutron detection. This study, as well as, information on the angular resolution, energy deposition, and photon/neutron identification will be reported here.

SIMULATION

Using simulation software available here at Jefferson Lab, the neutron detection efficiency was simulated. The simulation showed a neutron detection efficiency of about sixty percent once the efficiency came to a plateau. However, the real data may be different from the simulation, thus the real efficiency may not be what the simulation predicted.

GENERAL METHOD

The general method of determining the efficiency was to tag neutrons by a well known reaction: ep -> e'nπ^+ for which the detection of the e' and π^+ define the neutron momentum vector. Once this reaction has been identified a ratio method is used to find the exact efficiency: the ratio of the neutrons that were detected in the ep -> e'nπ^+ reaction to all the possible detections in the same reaction. Several cuts were made to try to unambiguously identify the e'nπ^+ final state. Through several particle identifications, fiducial, and angle cuts, an efficiency plot is produced with a high degree of accuracy.

Identifying the Final State Particles

ELECTRON AND PION IDENTIFICATION

Data from the Cerenkov counters and the large angle calorimeters, which identify electrons, were used to determine whether an electron was present in the final state or not. If an electron was detected, then the next step was to identify the π^+. If the charge on

another particle was positive, then that particle was determined to be either a proton, positive pion, or some other positively charged particle. Differentiating between particles was done by a hadron mass plot. Using the scintillation counter information on the time-of-flight, it was possible to evaluate the velocity of the particle once its trajectory was matched with its time-of-flight. The equation(1) used to determine beta (velocity/c) was:

$$\beta = \frac{L/(tof(h))}{c}$$

where L is the path length, and tof(h) is the time-of-flight for the hadron. Note that c equals 30.00 cm/nanosecond. Then from the β the mass was able to be determined in this manner (equation 2):

$$Mass = \frac{P}{\beta \times \gamma}$$

where P is the momentum of the hadron, and $\gamma = (1-\beta^2)^{-1/2}$. The hadron mass plot can be seen in Figure 1, which shows two prominent peaks. The first peak is from the π^+ which has a mass of 139.57 MeV, and the second is from the proton which has a mass of 938.27 MeV. Note that there are also two small peaks from K^+ (493.67 MeV) and D^+ (1868 MeV). So by making a cut on this plot from 0 GeV to 0.2 GeV, the π^+ in the final state has been identified.

MISSING MASS

Now that the electron and pion have been identified the neutron is the last particle to be determined in the final state. Relativistic kinematics shows that the square of the length of the four-vector momentum equals the mass squared (equation 3).

$$p^2 = \sum_u p_u{}^2 = -m^2$$

This relationship can be used to determine the missing mass of the reaction by solving for the momentum of the missing particle and squaring it, as shown here (equations 4 and 5) where $P = (\vec{p},E)$ for each particle, hence all P are four-vector momentums:

$$P_e + P_p = P_{e'} + P_\pi + P_x$$

$$P_x{}^2 = (P_e + P_p - P_{e'} - P_\pi)^2 = -m_x{}^2$$

Figure 1: Hadron Mass Plot

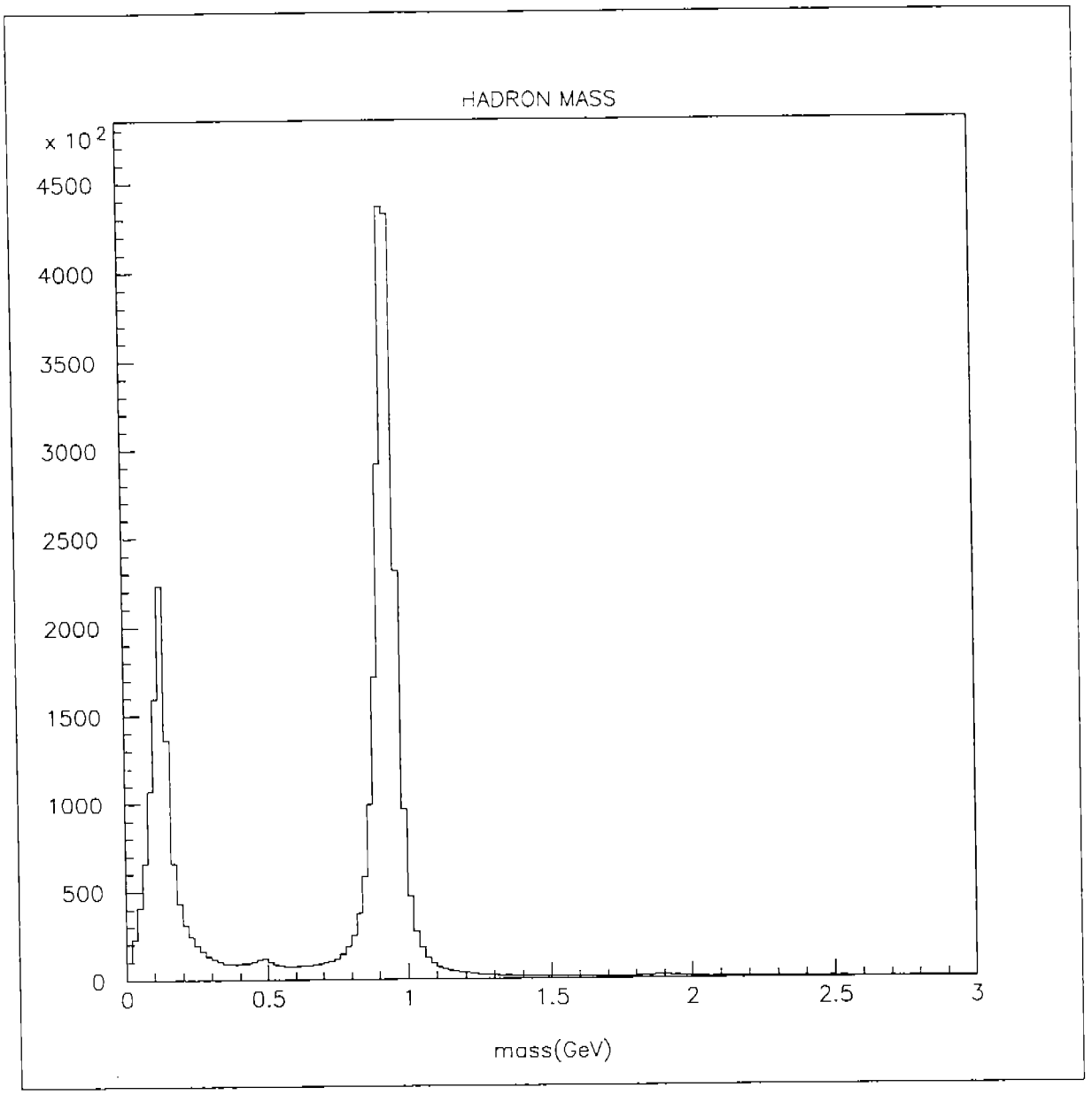

Note that the momentum vector ($\vec{p}$) of the proton is zero and the momentum of the electron in the initial state is zero in the x and y direction (the beam moves along the z-axis).

If a graph of this missing mass is now made it should reveal a peak at the neutron mass. Figure 2 shows this missing mass plot for neutrons that weren't detected, and Figure 3

shows the same plot for neutrons that were detected. In both plots there is a very visible peak at the mass of the neutron as well as some other contributions at higher masses. It is especially important when doing an efficiency study not to count events in which there actually was no neutron because the calorimeter would be deemed inefficient when it was not. Thus, it is essential to try and separate these other contributions, background, from actual neutrons. It is for this reason a cut was made on this graph to help ensure that only neutrons were being counted (this cut is superimposed in Figure 2 and was applied to Figure 3 although the plot does not show it), and this cut was made from .85 GeV to .95 GeV. To show that this cut is acceptable, Figure 4 is the same plot as Figure 3 except with a directional restriction (delta cut) applied to it, which will be described later. This shows that the missing mass cut is reasonable and that the surrounding contributions are not neutrons, but background, as predicted.

MISSING MOMENTUM

In the same manner that the missing mass was derived from the reaction, the missing momentum may be found. Recall equations four and five. From these equations it is possible to separate these vectors into their components to find the missing momentum in each direction (equations 6, 7, and 8) . Remember that the initial electron only has

$$p_{x_x} = -p_{e'_x} - p_{\pi_x}$$

$$p_{x_y} = -p_{e'_y} - p_{\pi_y}$$

$$p_{x_z} = E_{beam} - p_{e'_z} - p_{\pi_z}$$

momentum in the z direction and that the proton has no momentum only rest mass energy.

Now, these components can be added together to get the total missing momentum (equation 9).

$$P_x = \sqrt{p_{x_x}^{\ 2} + p_{x_y}^{\ 2} + p_{x_z}^{\ 2}}$$

FIDUCIAL CUTS

Using the missing momentum vectors, the direction of the neutron is able to be determined. Simply dividing each x, y, and z component of the missing momentum by the magnitude of the whole momentum vector yields the unit missing momentum vector (cosine x, cosine y, and cosine z), in other words the direction of the neutron in the x, y, and z directions.

Figure 2: Missing Mass Plot (for undetected neutrons)

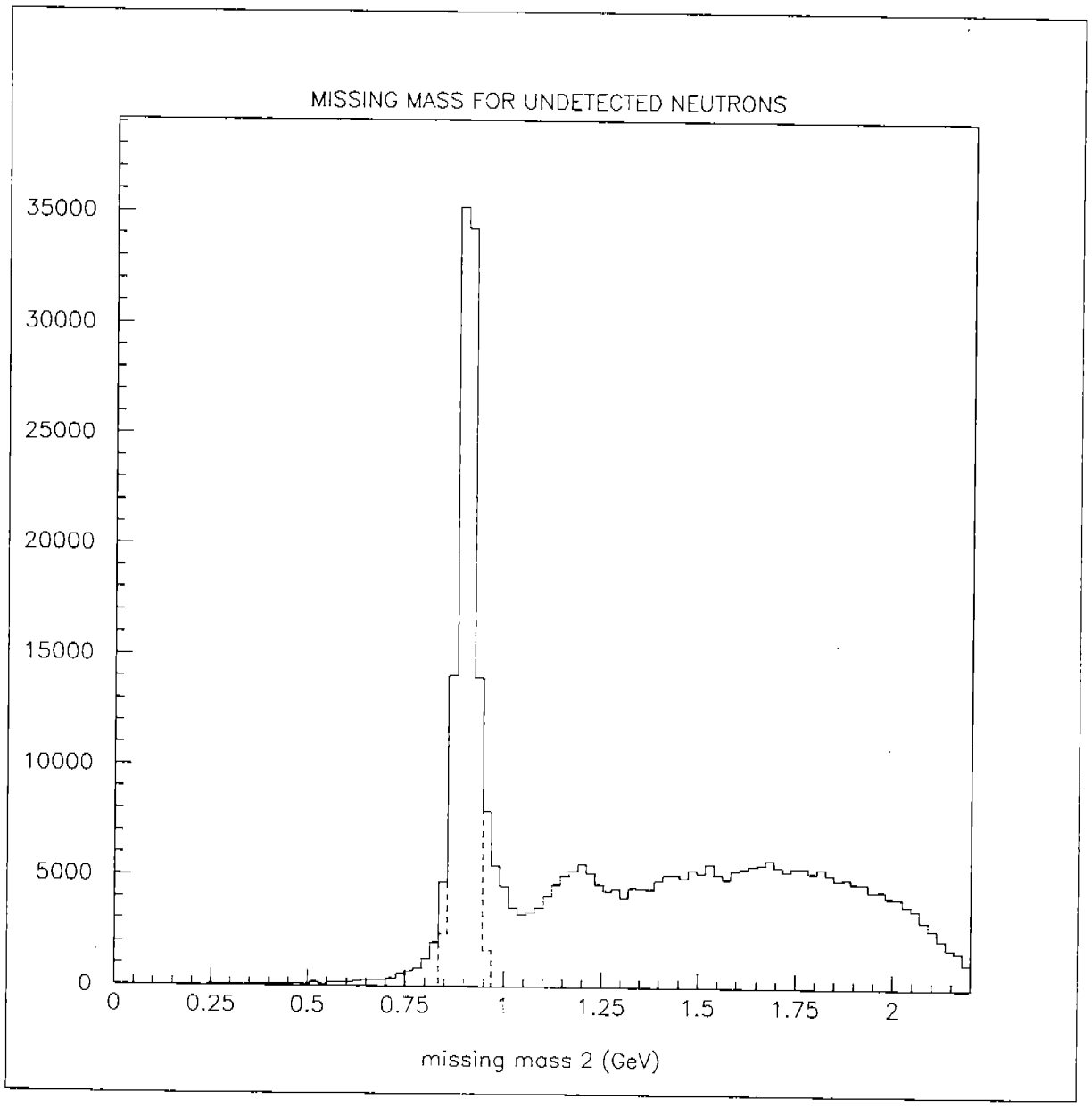

Figure 3: Missing Mass Plot (for detected neutrons)

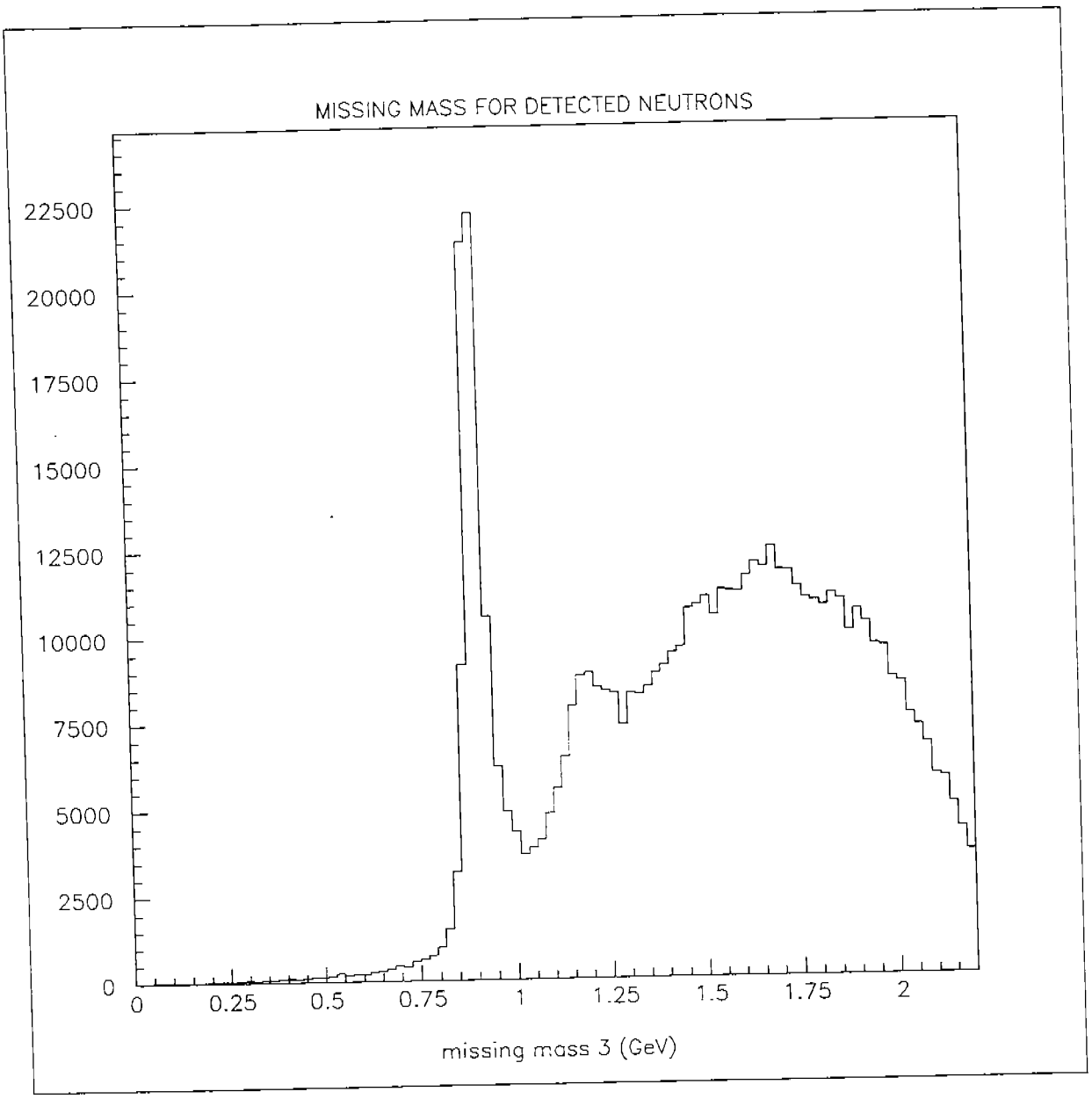

Figure 4: Missing Mass Plot for detected neutrons with a directional cut applied

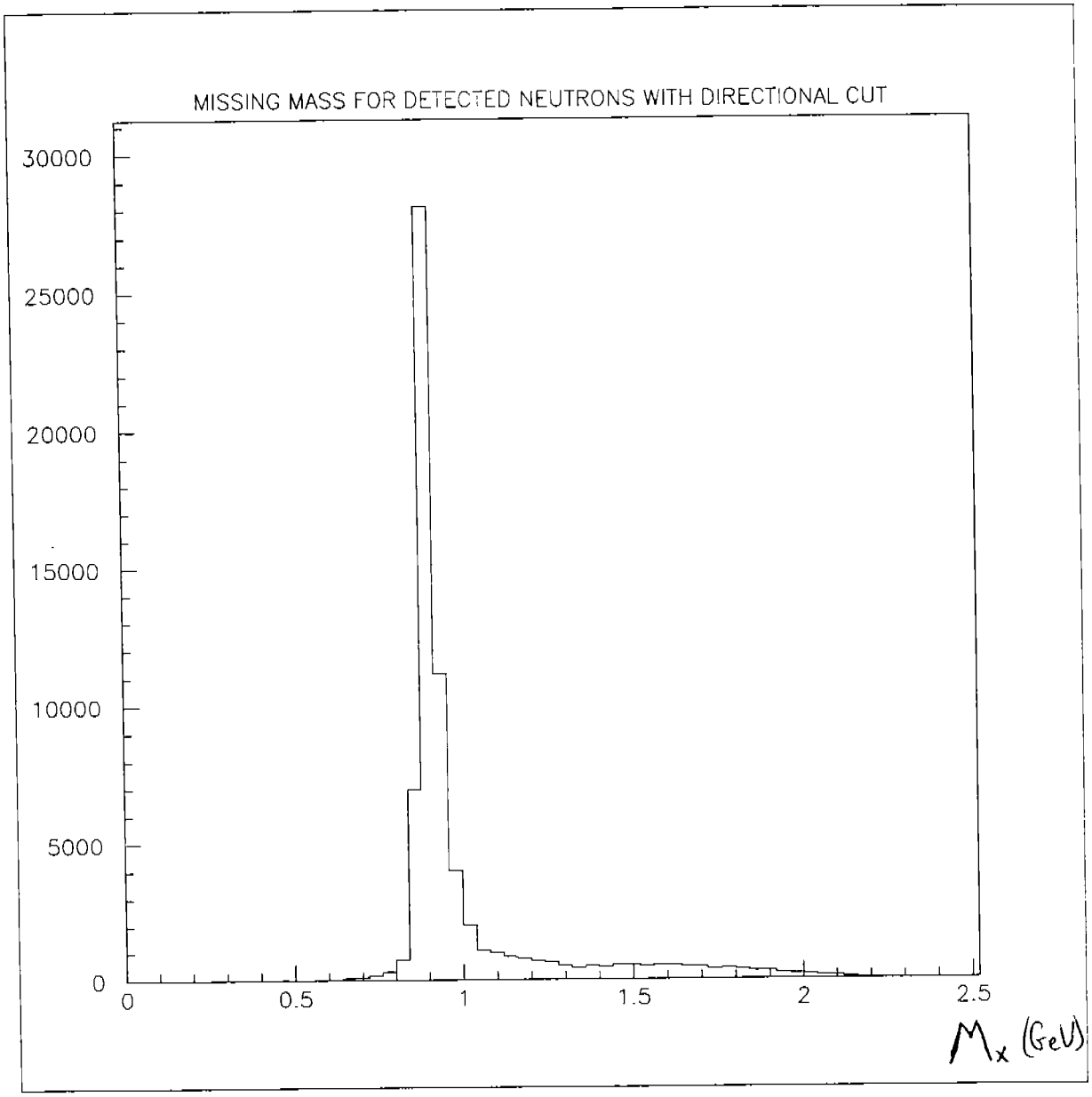

Now it is quite obvious that the unit missing momentum vectors can and will go is all directions (Figure 5). Notice in Figure 5 that there is a high neutron concentration around the beam direction, thus most neutrons are scattered at very small angles.

Figure 5: Uncut Missing Momentum Direction (cosine x vs. cosine y of missing momentum)

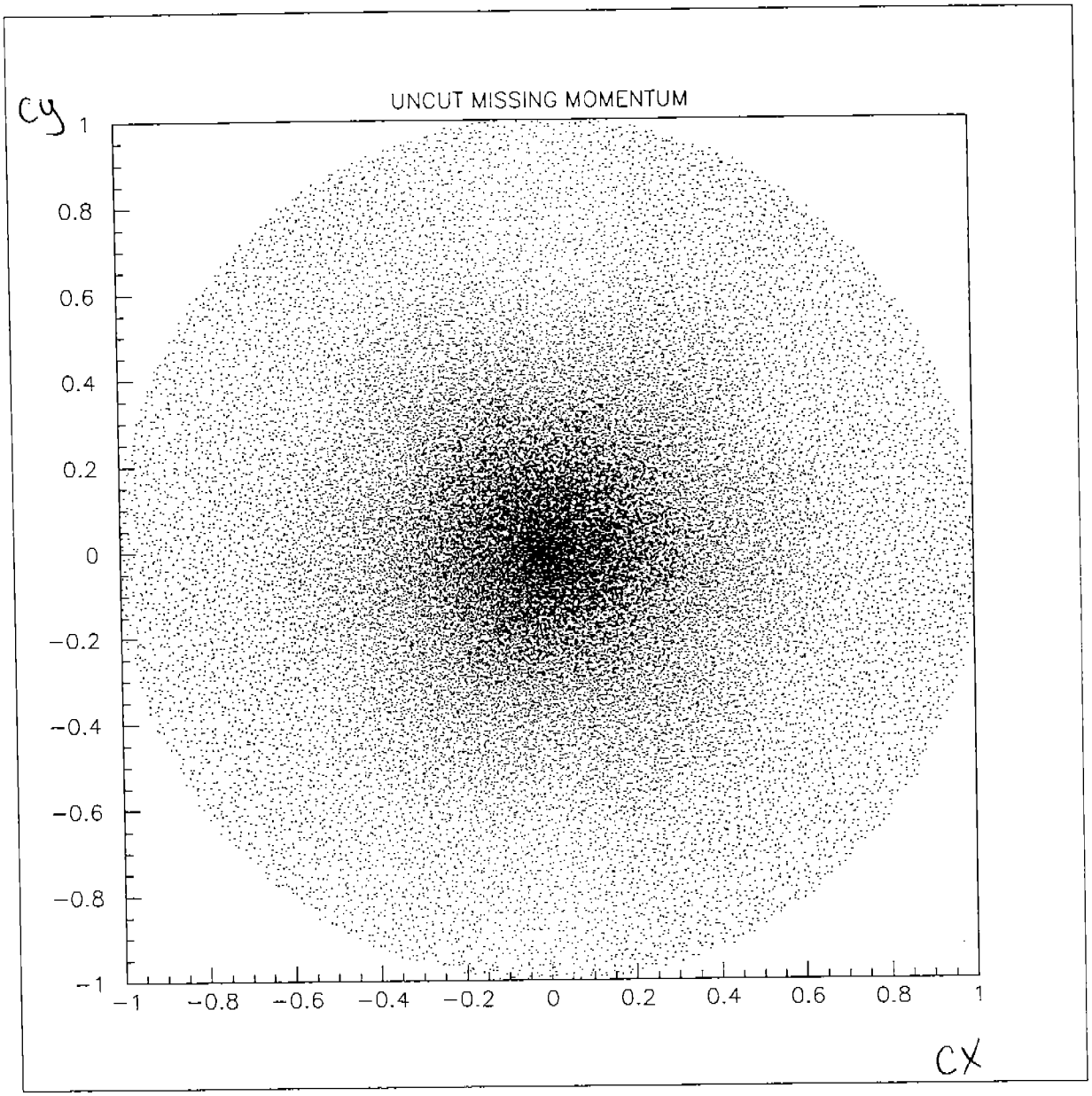

The structure of CLAS prevents neutrons from being detected in all directions. As mentioned before, inside CLAS there are six superconducting coils which limit the capability of the calorimeter to detect neutrons. By this I mean, if a neutron's momentum is in the direction of a coil it can be lost, thus the calorimeter never even had the chance to detect it. It is for this reason that several coil cuts were made so that these neutrons that were directed toward the coils are not counted as an inefficiency in the calorimeter. By

looking at a plot like Figure 5 for neutrons that actually were detected the positions of the coils become very apparent (Figure 6).

Figure 6: Direction of *actual* neutrons found by the detector (cosine x vs. cosine y)

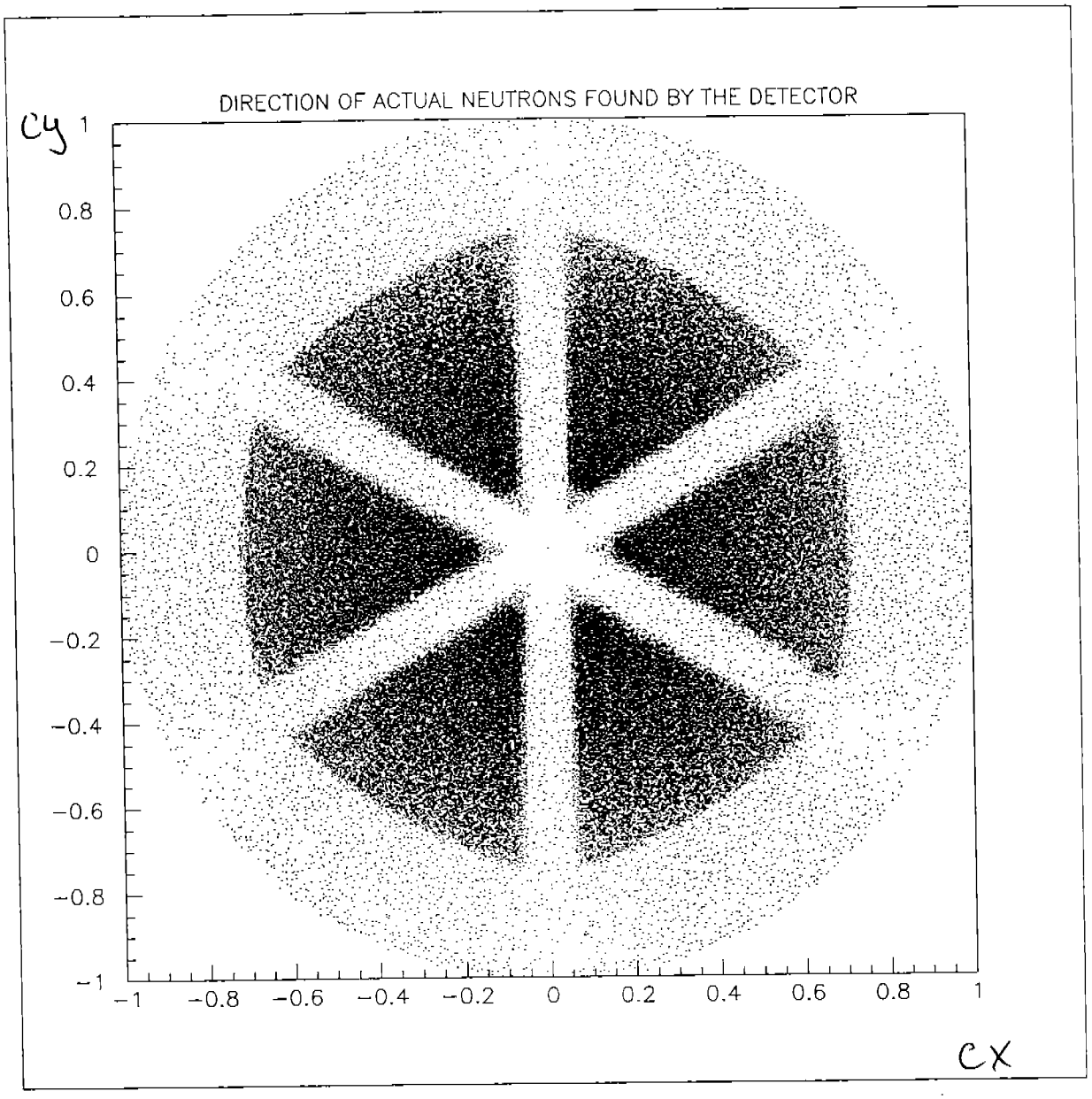

Now by defining three lines where the six coils are positioned and giving a width to these lines, three cuts are able to describe the obstruction caused by the coils. Note that

all the vectors that these cuts were made on were the unit vectors of the momentum, hence this cut is directional. These three lines are (equations 10, 11, and 12):

$$\hat{p}_y = \frac{-\sqrt{3}}{3} \cdot \hat{p}_x \pm \frac{w}{\cos 30}$$

$$\hat{p}_y = \frac{\sqrt{3}}{3} \cdot \hat{p}_x \pm \frac{w}{\cos 30}$$

$$\hat{p}_y = \pm w$$

where w is the width (0.075) of the line. Therefore, by requiring p_y to be greater than the line plus the width and less than the line minus the width, the coil cuts are executed.

In addition to the coils the calorimeter itself creates a restraint on its ability to detect neutrons. From the z plane, each calorimeter only reaches forty-five degrees above it, or in other words can only detect up to a theta of forty-five degrees. Again recall Figure 6, a clear boundary is seen around the outside in comparison to Figure 5. This radius is the limit of the calorimeter. This is why a radial cut was also implemented. This radial cut appears like this $\hat{p}_x^{\,2} + \hat{p}_y^{\,2} < R^2$, where R is the radius (0.7). These two cuts, radial and coil, applied to the calculated missing momentum unit vectors gives these plots, Figure 7 for neutrons that weren't detected and Figure 8 for neutrons that were detected.

Also note that this radial cut parallels a theta cut since,

$$1 = \sqrt{\hat{p}_x^{\,2} + \hat{p}_y^{\,2} + \hat{p}_z^{\,2}}$$

$$r = \sqrt{\hat{p}_x^{\,2} + \hat{p}_y^{\,2}}$$

$$1 = r^2 + \hat{p}_z^{\,2}$$

$$\cos\theta = \frac{p_z}{\vec{p}} = \frac{p_z}{1} = \hat{p}_z$$

$$r = \sqrt{1 - (\cos\theta)^2}$$

$$r = \sin\theta$$

These two cuts also provide two new parameters w, width, and R, radius, which can easily be adjusted to any desired value. This is important because when they are changed their effects can be seen immediately without much work.

Once all of these cuts had been applied a plot of the missing momentum was made (Figure 9). This plot reflects the momentum of the neutrons that were not detected. The missing momentum plot for the detected neutrons will be made after one more additional cut.

Figure 7: Missing Momentum Direction with radial and coil cuts (cosine x vs. cosine y)

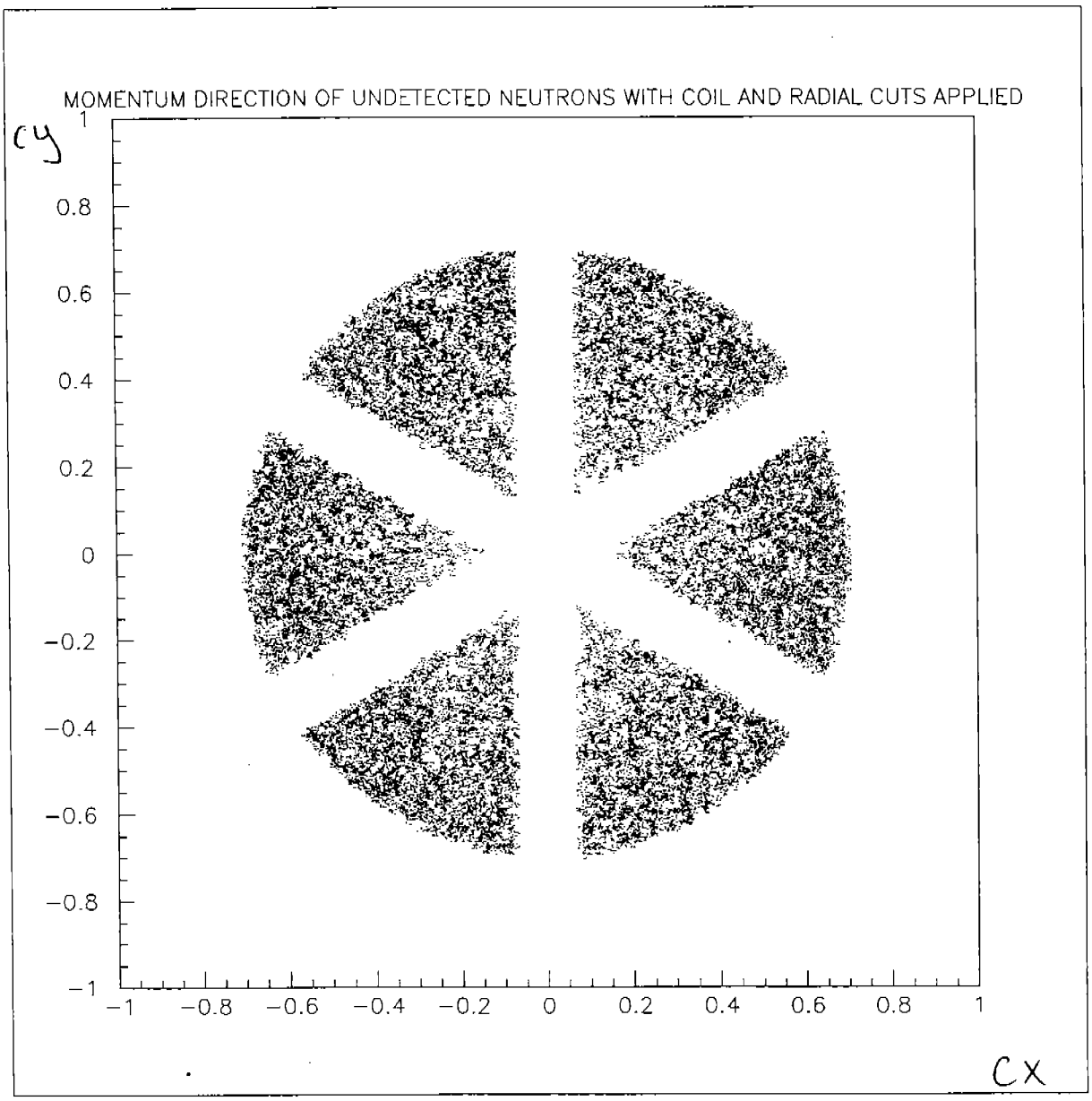

Figure 8: Missing Momentum Direction with radial and coil cuts (cosine x vs. cosine y)

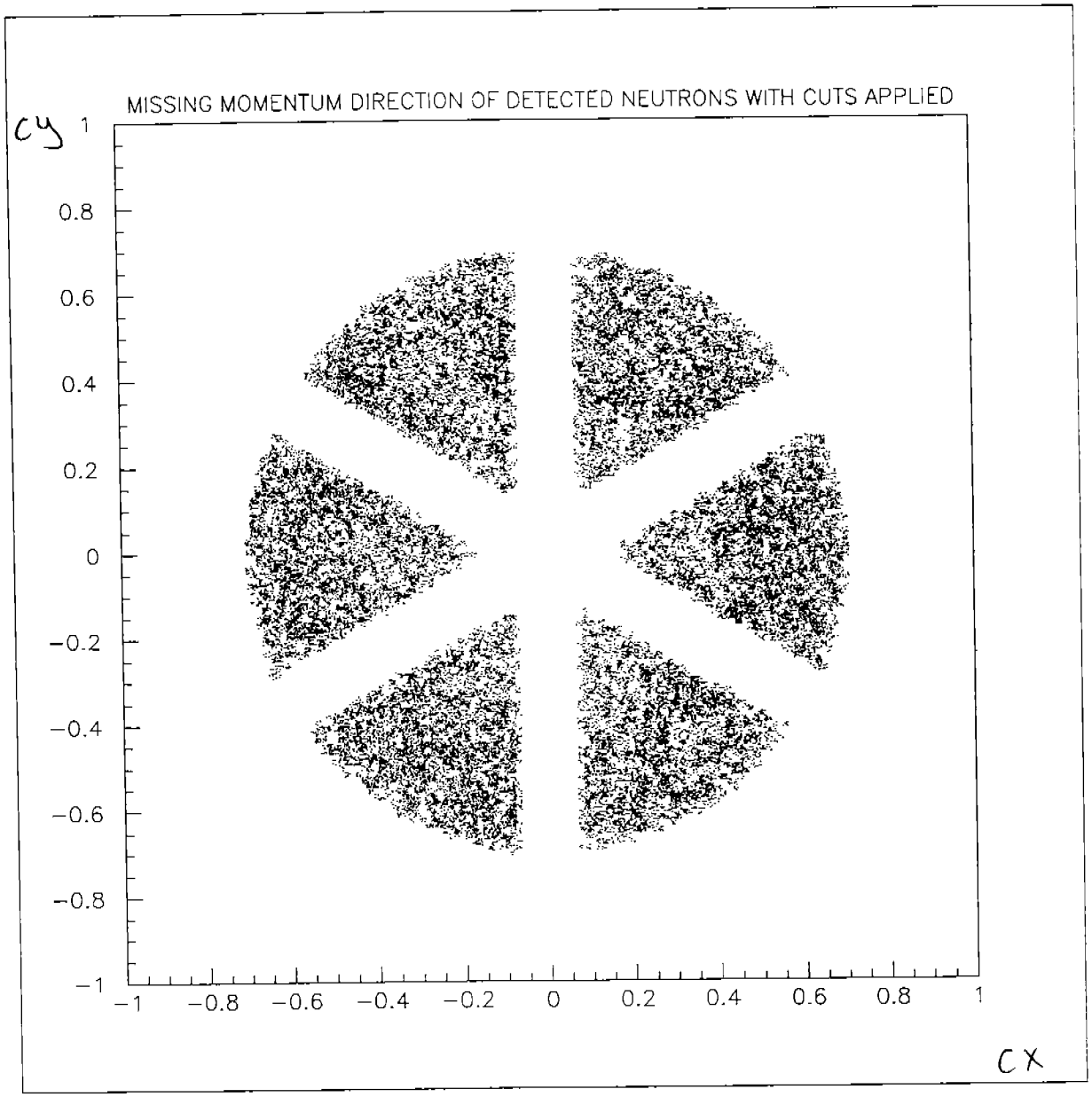

Figure 9: Missing Momentum when CLAS detected e' and π^+

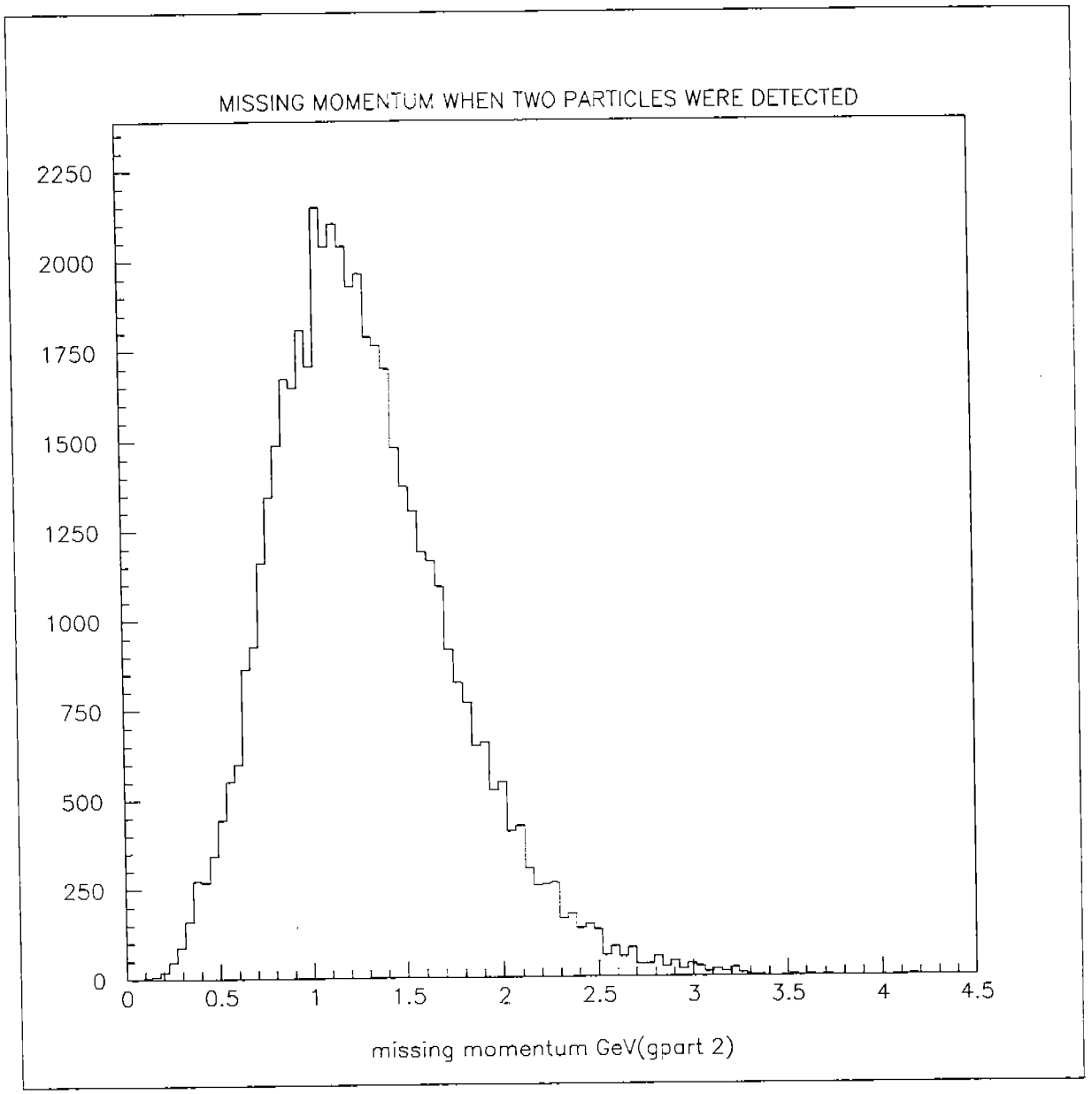

Detected Neutrons Only

DELTA CUTS

When the calorimeter records a hit, it is able to provide information on the position of that hit. It is able to give data on the unit momentum vector, in other words, the direc-

tion it believes it came from. Finding the unit vectors of the missing momentum should provide the same information. When there is a discrepancy between these two values, then something is wrong. For example, if the detector reports it saw a neutron but it was really a photon its unit vectors would not match the missing momentum unit vectors found for the neutron. In Figure 10 this can be more clearly understood.

Figure 10: Delta Cosine x vs. Delta Cosine y

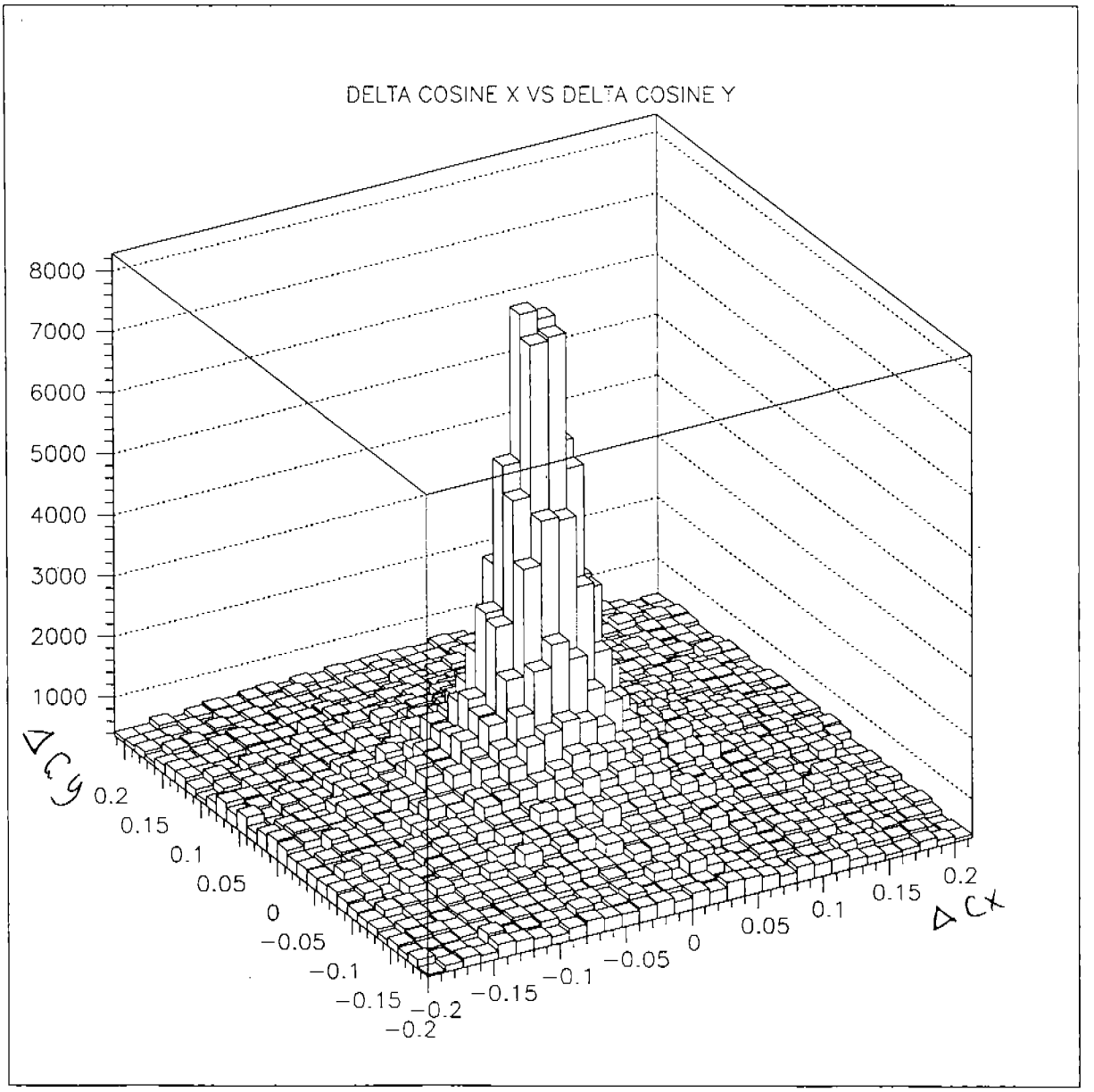

(Note that this plot has *no* cuts on it.) All of the background around the central peak at zero most likely can be explained by phenomenon of this sort. Thus a cut is placed on these delta (delta between actual and predicted) values of cx and cy (unit momentum vectors in the x-direction and y-direction). This cut was a radial one appearing as $\Delta\hat{p}_x^{\,2} + \Delta\hat{p}_y^{\,2} < r^2$, where r is equal to .05. Figure 10 after the cut (Figure 11) has one large peak at zero and almost all of the background has been eliminated.

Figure 11: Delta Cosine x vs. Delta Cosine y with the cut applied

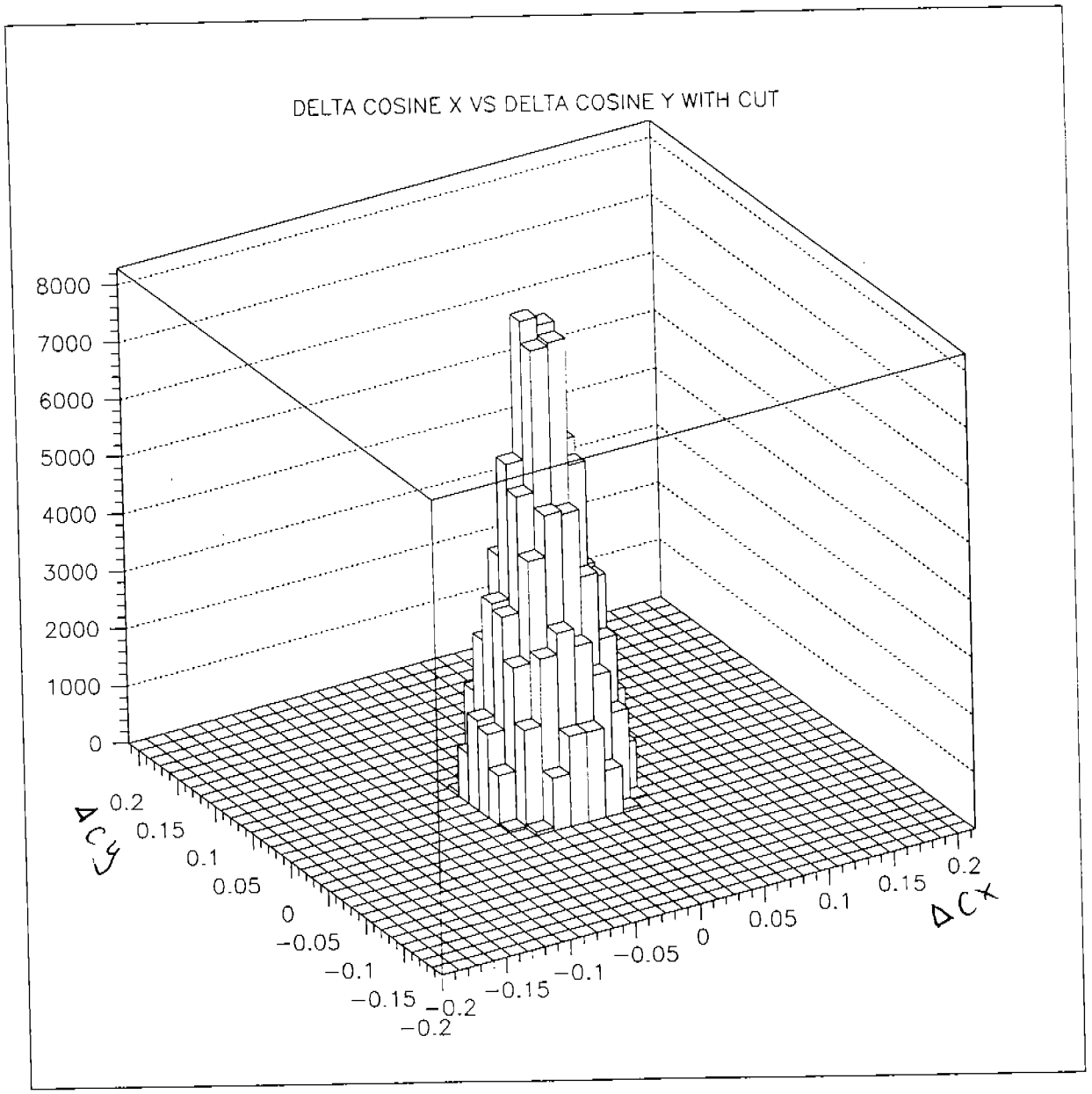

Once all of these cuts had been applied like before a missing momentum plot was made (Figure 12).

Figure 12: Missing Momentum for Detected Neutrons

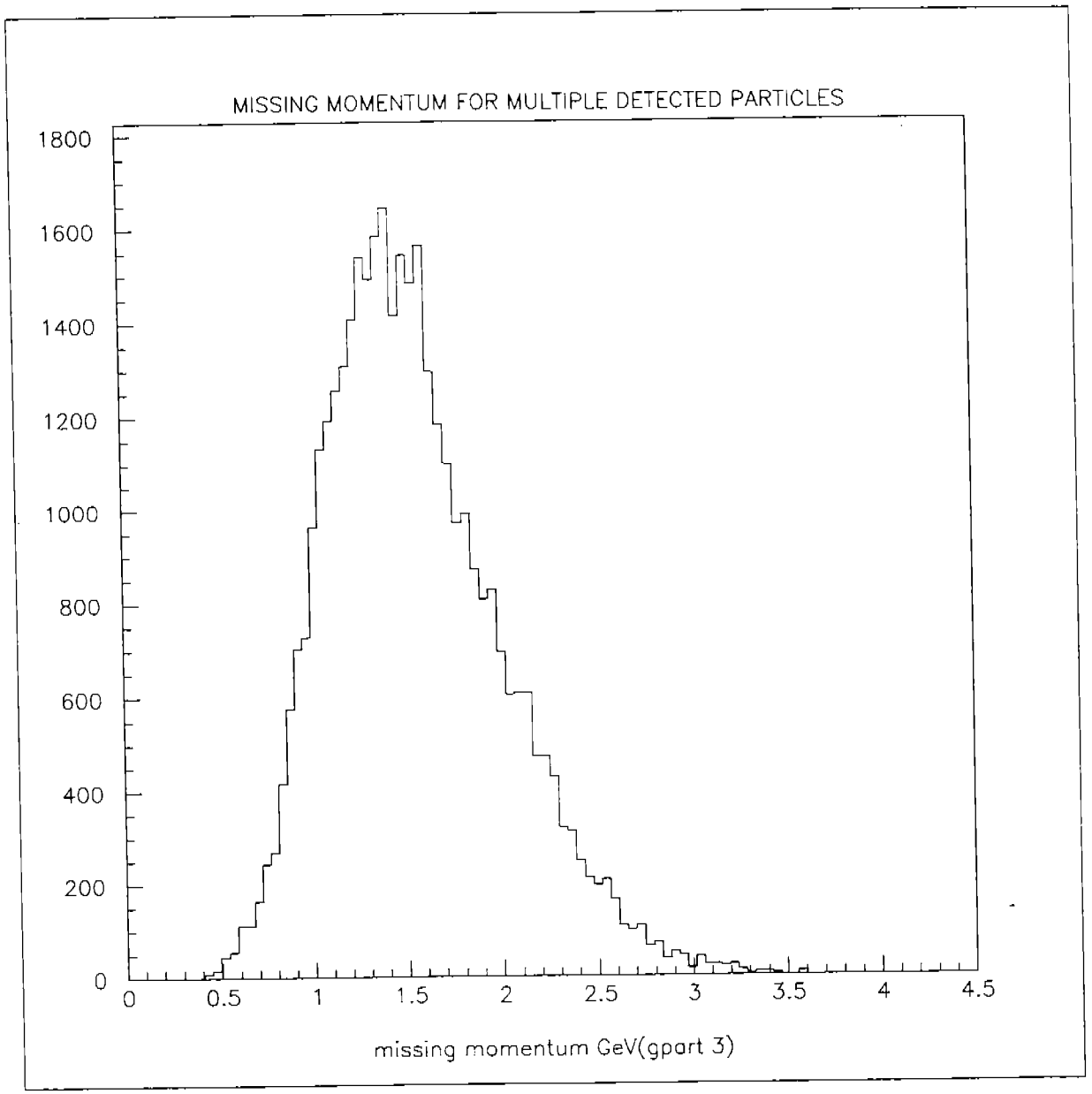

Hence, this plot contains neutrons that were detected.

Summary of Cuts

TABLE 1. Summary of all cuts made prior to each missing momentum plot

CUTS	UNDETECTED NEUTRONS	DETECTED NEUTRONS
hadron mass	X	X
0.0<mass<0.2		
missing mass	X	X
0.85<mass<0.95		
coils	X	X
width=0.075		
calorimeter radial (theta)	X	X
radius=0.7		
delta cuts		X
radius=0.05		

(Refer to previous pages for a detailed description of each cut)

Efficiency

Now if the two missing momentum plots are added together the result is a plot of all possible neutron detections (Figure 13). Using this plot and the plot of the missing momentum of the detected neutrons, an efficiency plot is easily obtained by simply taking the ratio of these two plots with the missing momentum plot of the detected neutrons as the numerator. In order to make this plot as accurate as possible an error calculation for the efficiency was made. It was calculated as follows (equation 13):

$$\sigma = \frac{\sqrt{(N-1)\times R\times(1-R)}}{(N-1)}$$

where R is the ratio and N is the total number of possible neutron identifications. Figure 14 shows the efficiency plot with this error calculation included. It can be seen that the efficiency increases with, increasing neutron momentum, and plateaus at about sixty percent as the simulation predicted.

Figure 13: Missing Momentum of all possible neutron identifications

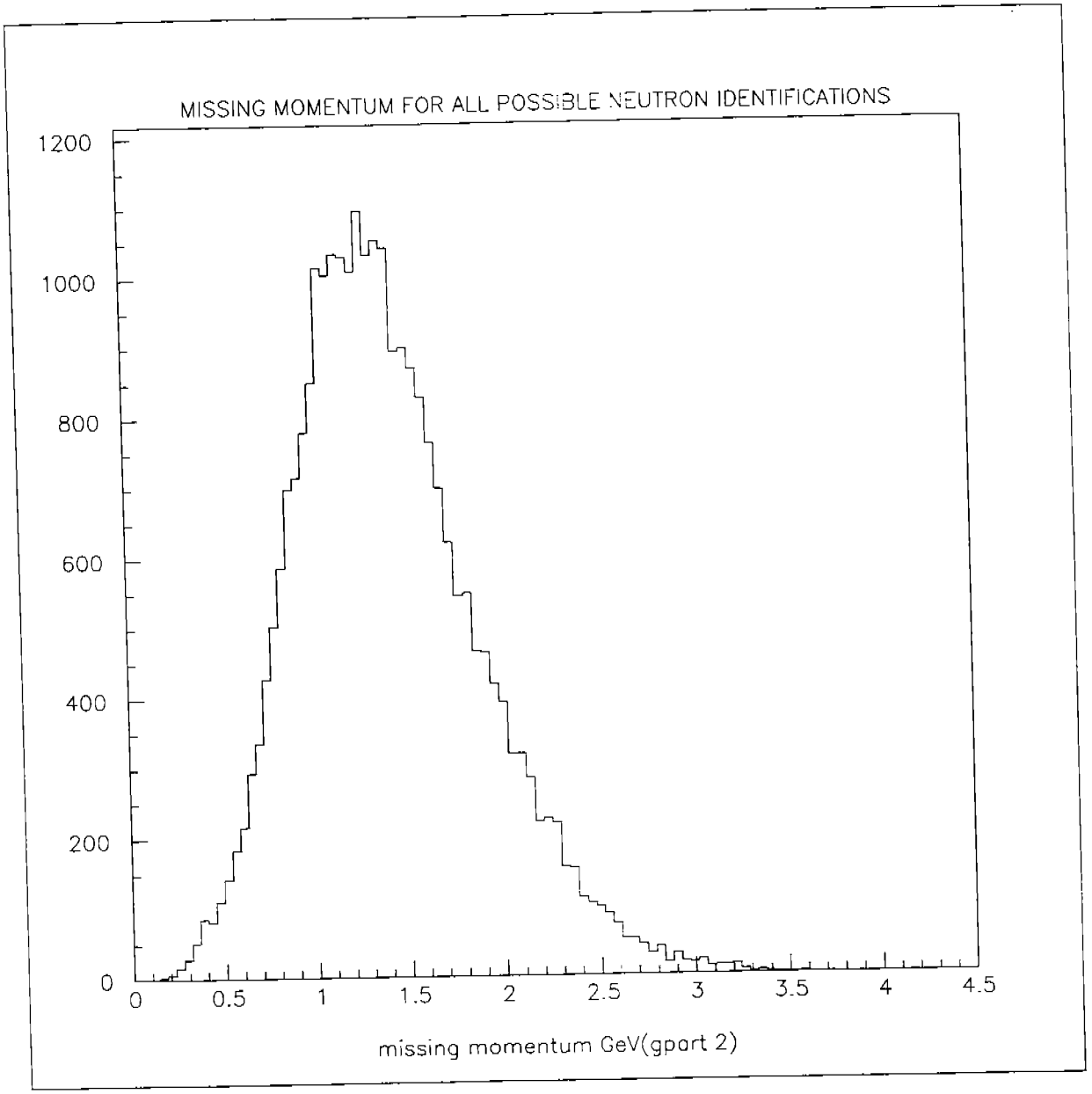

Figure 14: Neutron Detection Efficiency

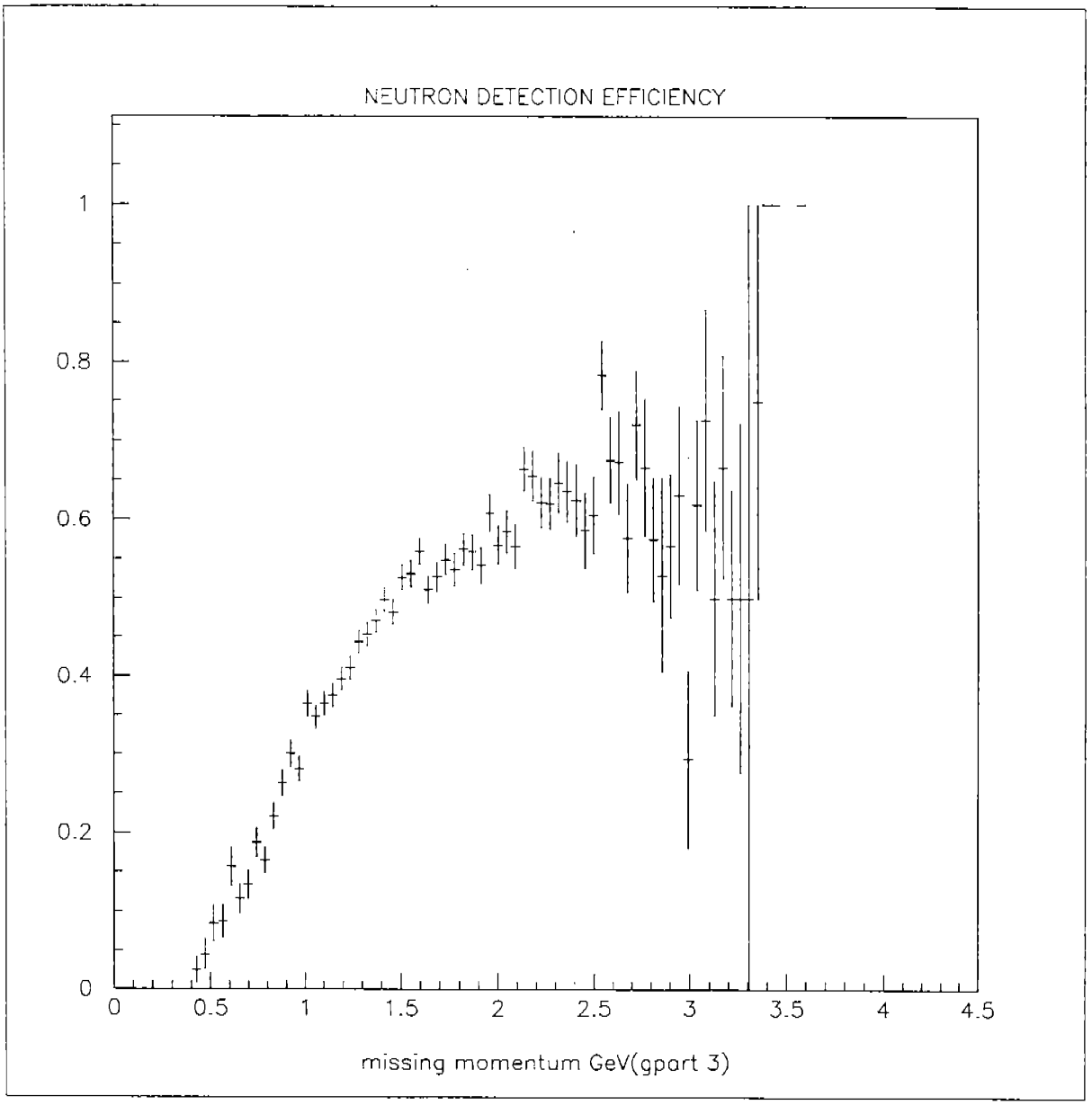

Beyond Neutron Detection Efficiency

ANGULAR RESOLUTION

In addition to determining the efficiency of the forward calorimeter to detect neutrons, the angular resolution for neutrons was also examined. From the information provided by the electron and π^+ in the drift chambers a predicted neutron angle can be determined. As derived before from the electron and π^+, the missing momentum components can be found. Once these vectors are put into unit vector form the predicted θ and ϕ angles may be calculated (equations 14 and 15).

$$\theta_p = \text{acos}(\hat{p}_z)$$

$$\phi_p = \text{atan}\left(\frac{\hat{p}_y}{\hat{p}_x}\right)$$

The θ and ϕ from the calorimeter may be found by the same equation except the unit vector of the missing momentum is removed and the unit vector the calorimeter found replaces it. Now taking the difference between these two values gives $\Delta\theta$ and $\Delta\phi$. Figures 15 and 16 show $\Delta\theta$ and $\Delta\phi$ versus momentum. By slicing these plots and projecting them onto the y-axis a plot of $\Delta\theta$ and $\Delta\phi$ is seen for particular momentums. If each of these projections are fit with a gaussian distribution a sigma is obtained for each. Each of these sigmas are plotted versus momentum with the weighted error assigned by PAW to produce the angular resolution plots (Figures 17 and 18). These plots show that the θ resolution improves with increasing momentum and reaches about a half of a degree resolution. The ϕ resolution behaves the same except it only reaches a resolution of about a one and a quarter degree. Note that the error on the last point for the ϕ resolution plot is most likely due to a lack of statistics.

ENERGY DEPOSITS

Another aspect of neutron detection that was briefly examined was the manner in which the neutron deposits its energy in the calorimeter. Figure 19 shows a plot of the energy deposit in the front of the calorimeter versus the energy deposited on the rear of the calorimeter. The interesting aspect of this plot is that it appears that most of the neutrons deposit almost all of their energy either in the front or rear of the calorimeter but few deposit it over both.

Figure 15: Delta Theta vs. Missing Momentum

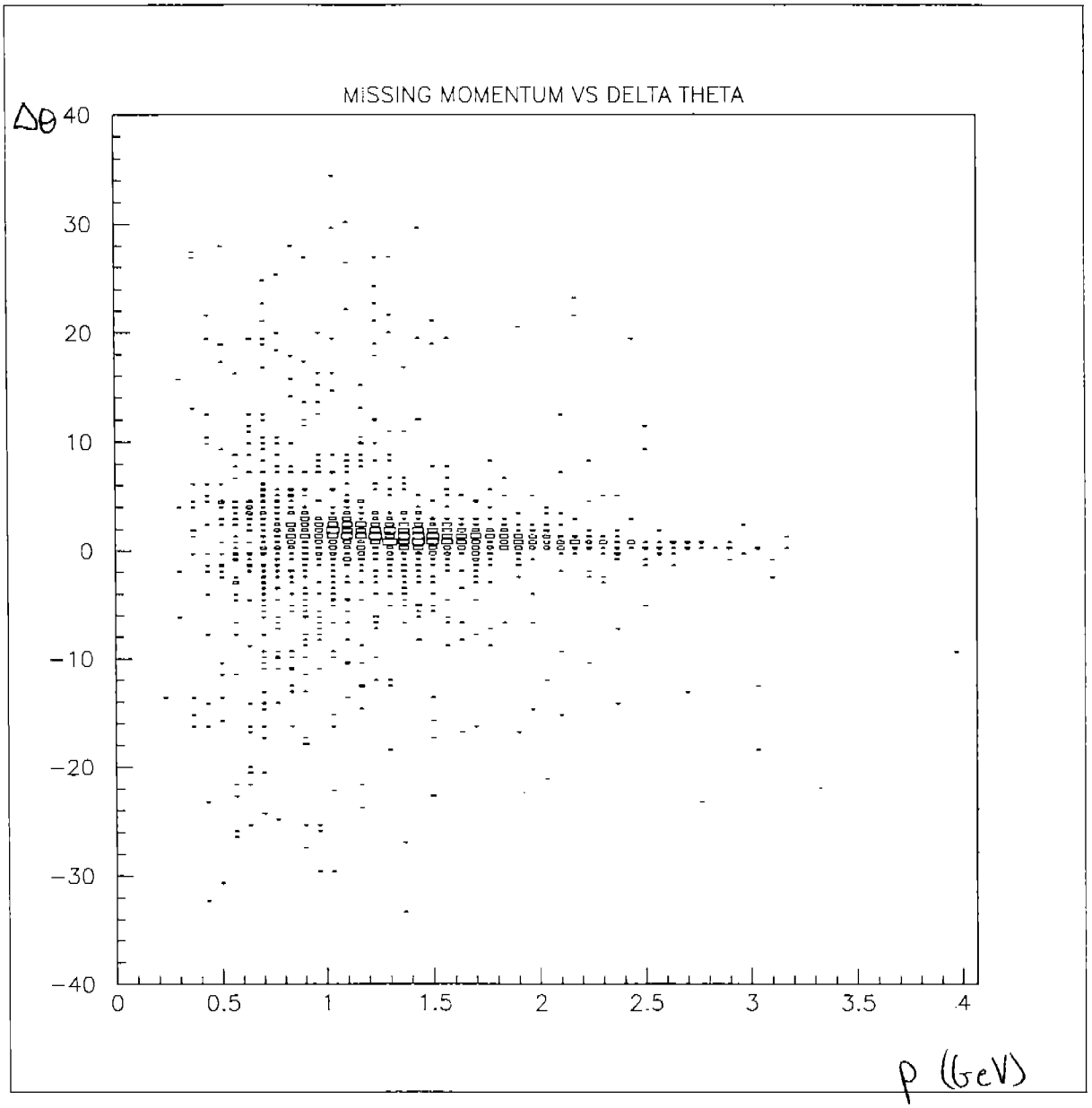

Figure 16: Delta Phi vs. Missing Momentum

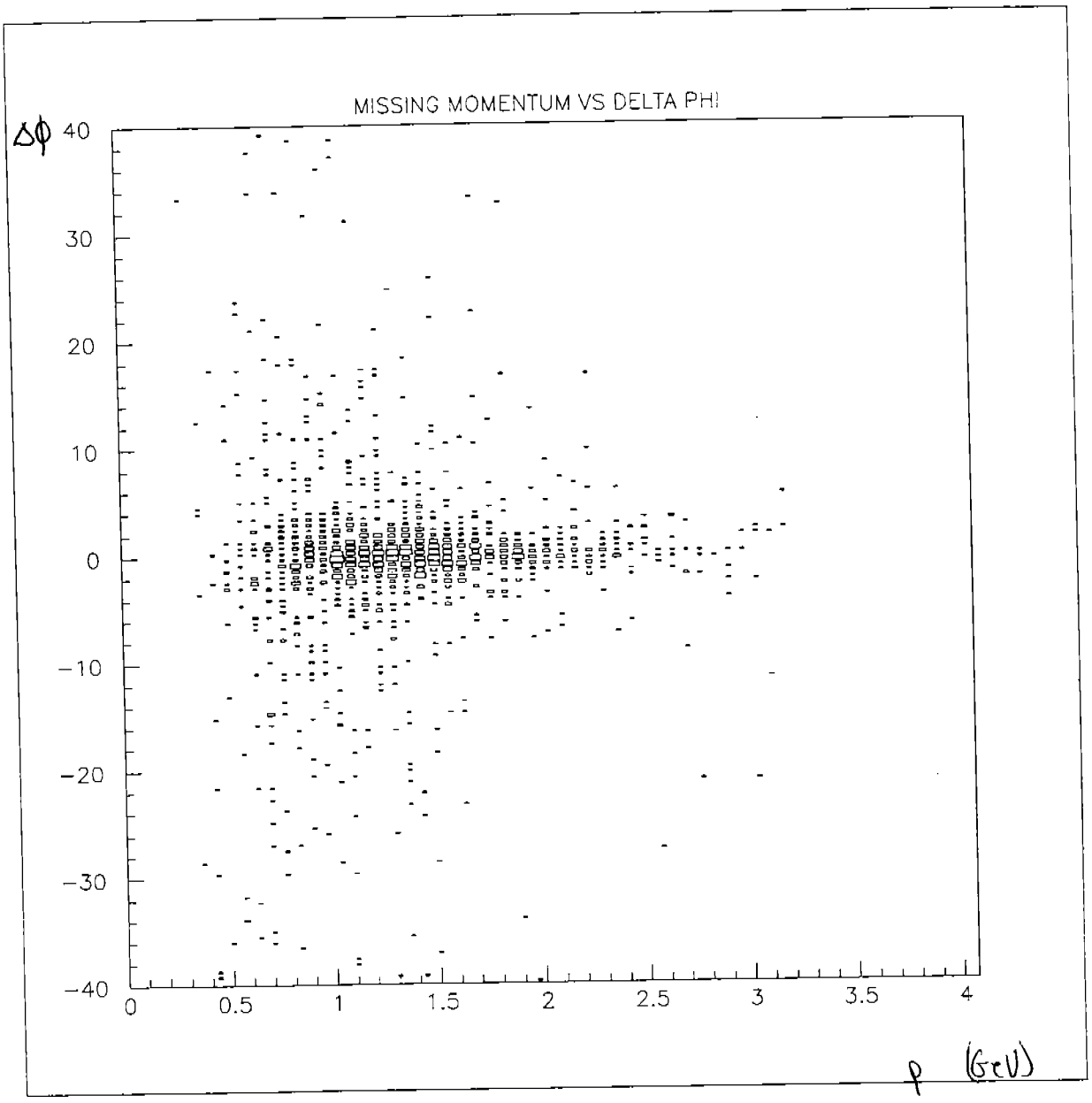

Figure 17: Theta Resolution vs. Missing Momentum

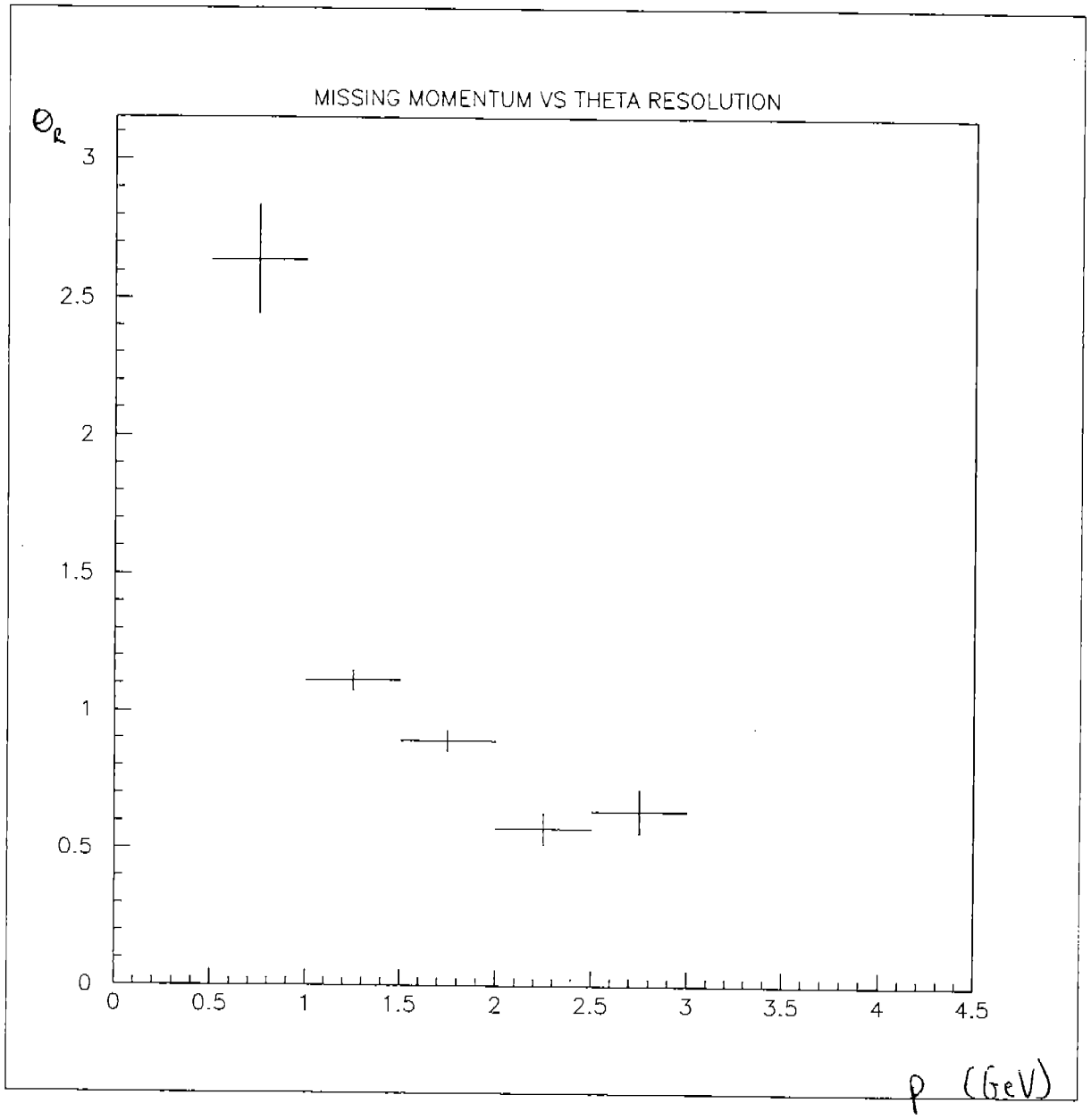

Figure 18: Phi Resolution vs. Missing Momentum

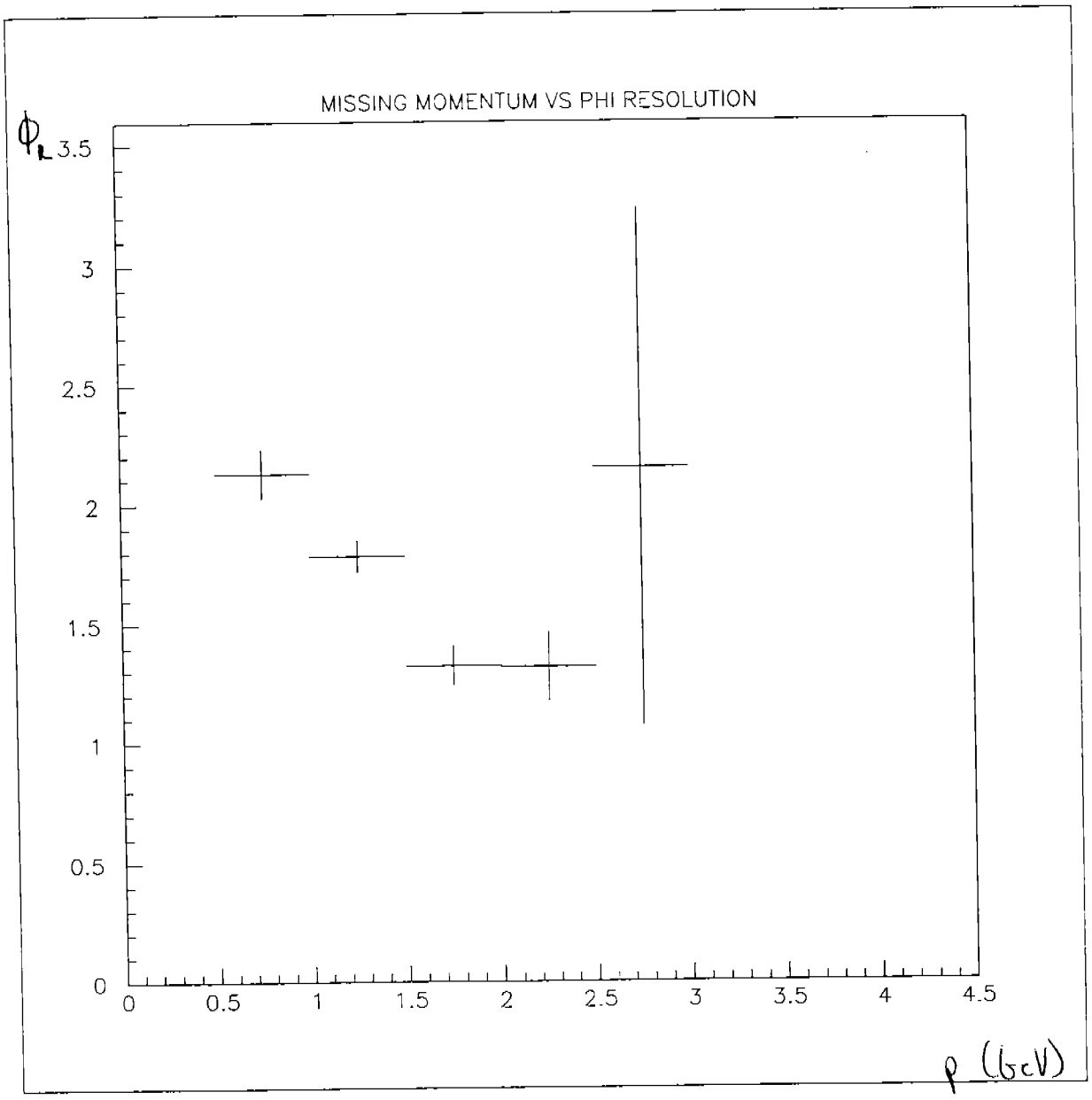

Figure 19: Energy deposited in the front of the calorimeter vs. Energy deposited in the back

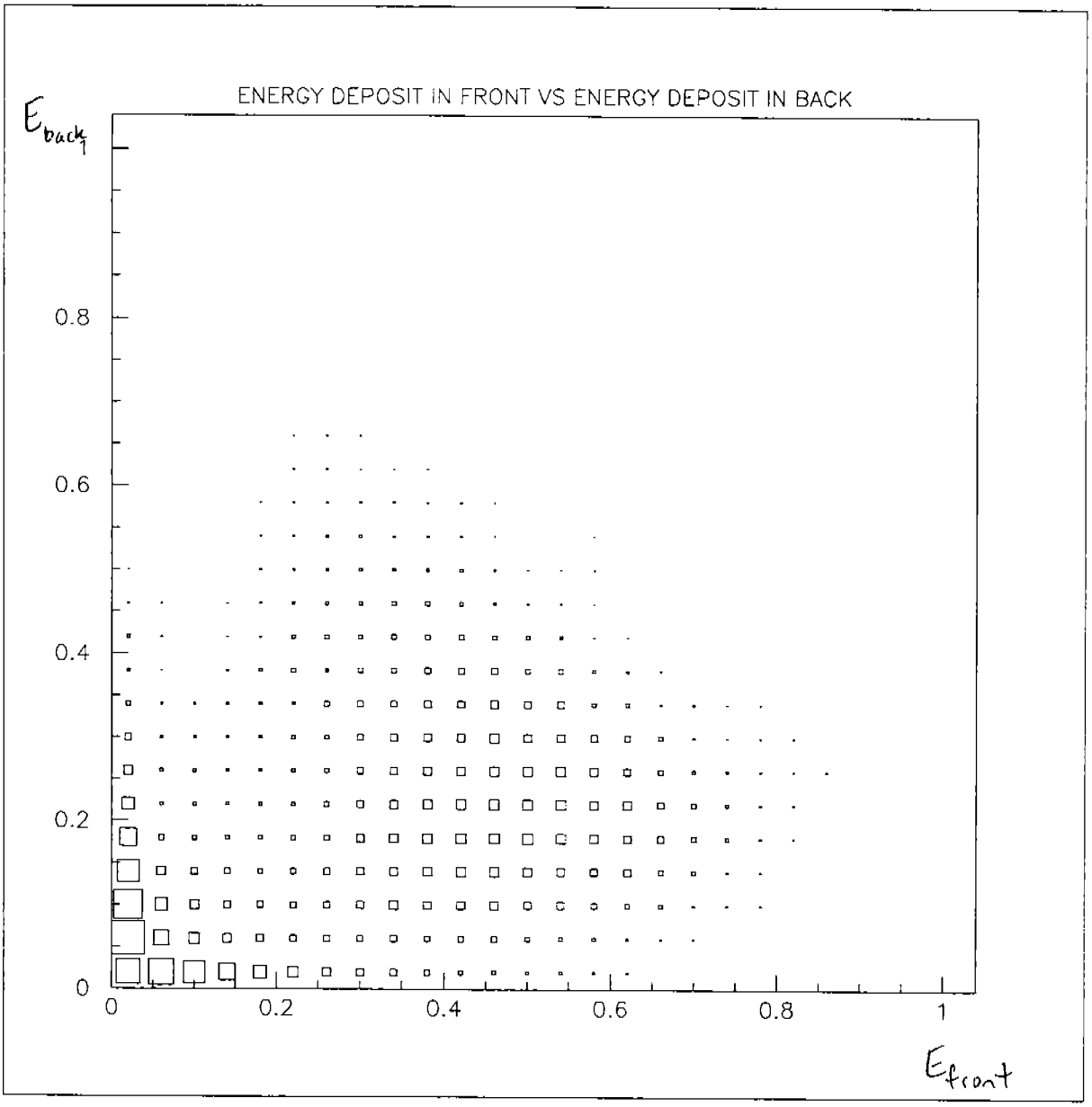

PHOTON/NEUTRON SEPARATION

In addition to the resolution and energy deposits an attempt was made to separate photons from neutrons using time to determine velocity.

Using the ep->e'pγ and the ep->e'pπ^0 reactions a calibration of the timing variables given by the calorimeter was attempted. Like before with the neutrons a hadron mass plot was made but instead of making the cut around the pion it was made around the proton from .88 GeV to 1.00 GeV. Then by substituting in the proton from the final

state for the pion in the neutron reaction a missing mass plot is made in the same manner as before (Figure 20). A cut was put on this plot from -.05 GeV to .05 GeV.

Now beta is solved for using this equation(16):

$$\beta = \frac{L/(tof(photon))}{c}$$

where L is the radial path length of the photon, tof(photon) is its time-of-flight, and c equals 30.00 cm/nanosecond. If a plot of beta is made at this point it will be noticed that the peak is not at one as it should be since photons move at the speed of light. This error is due to the poor calibration of the timing in the calorimeter. The tof(photon) is found in this manner (equation 17):

$$tof(photon) = tof(e) - tdc(e) + tdc(photon)$$

where the time-of-flight of the electron is $tof(e) = L/c$ (L is its path length and c is 30.00 cm/nanosecond), tdc(e) is the time for the electron after the trigger, and tdc(photon) is the time for the photon after the trigger. This tdc(photon) value comes from a variable found by the calorimeter called ec_t and this is the variable that is poorly calibrated. Since it is known that photons move at the speed of light, its predicted time can be easily found by (equation 18):

$$t_1 = \frac{L}{c}$$

where L is the photon's radial distance, and c equals 30.00 cm/nanosecond. Therefore, the difference between this time and the tof(photon) found by the calorimeter would be the correction time. This correction was then applied to each photon, and the position determined by the unit momentum vectors given by the calorimeter were also recorded for each photon that was corrected. Thus a time correction that is dependent on position was determined. With this correction applied a new β plot was made (Figure 21). The peak of this graph is now positioned correctly, however this peak is rather wide. For this reason, a plot of the time resolution was made, in other words, a plot of Δt (time) (Figure 22).

Figure 20: Missing Mass Plot for the Calibration Reaction

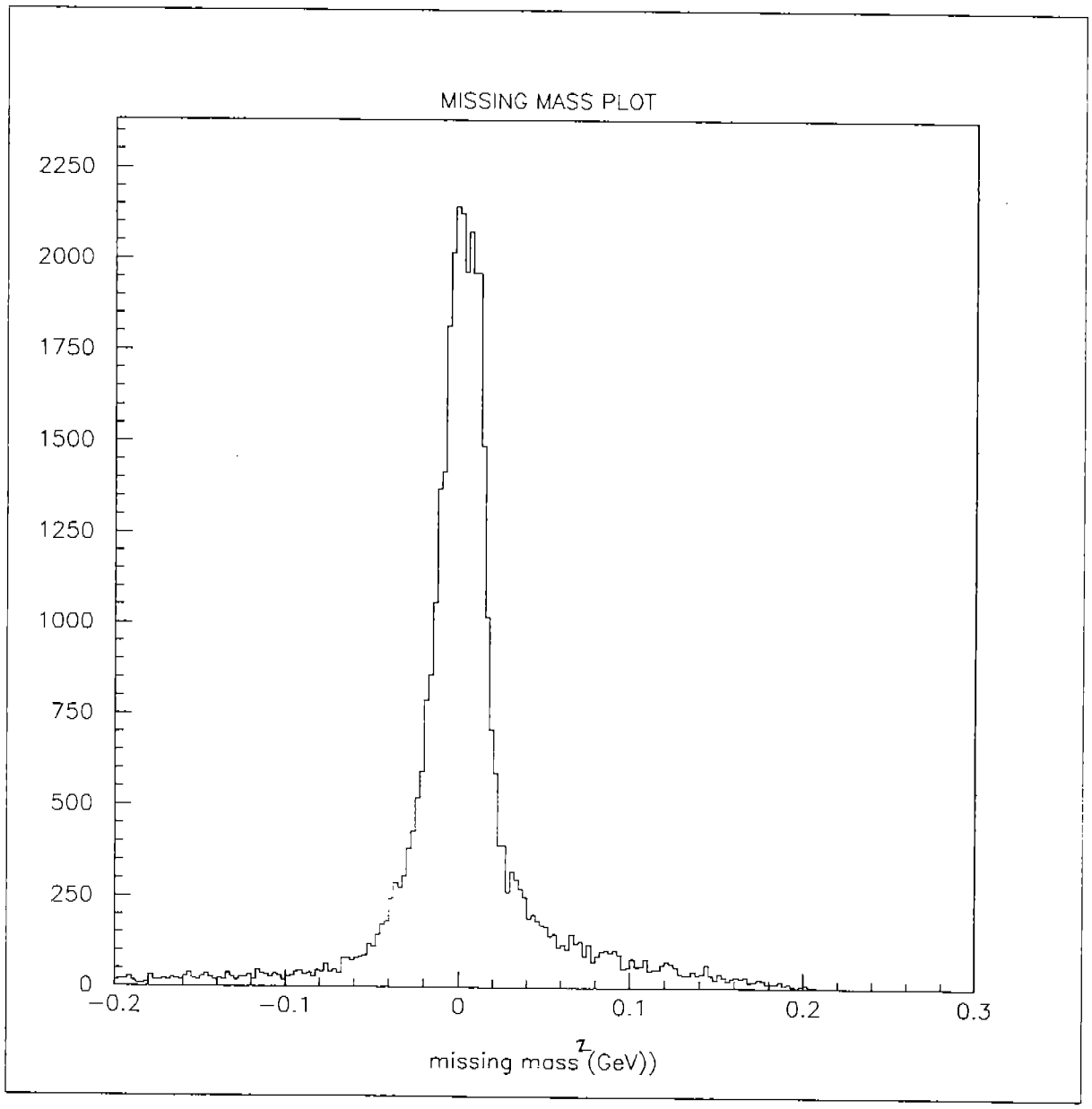

Figure 21: β for Photons

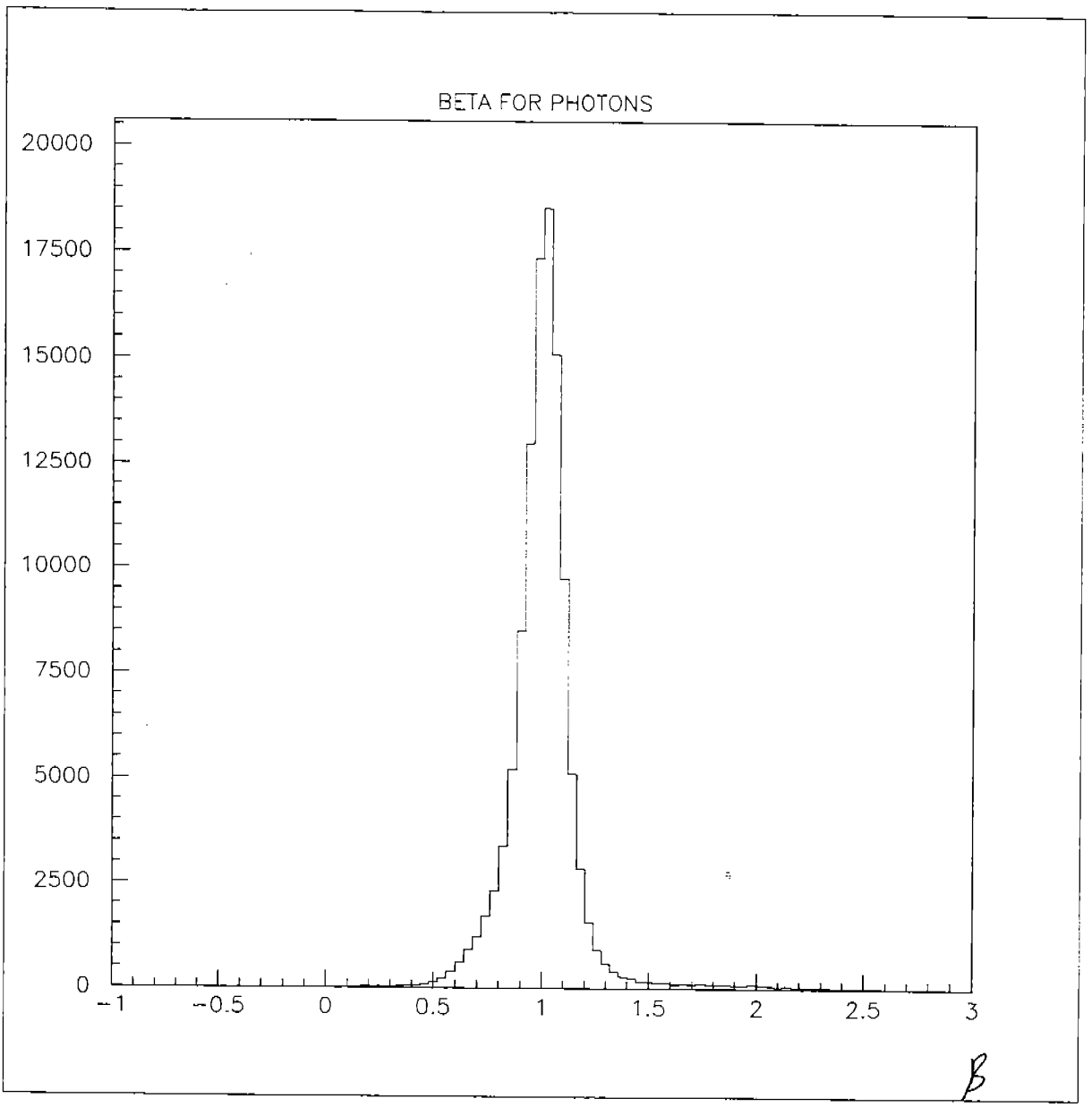

Figure 22: Time Resolution

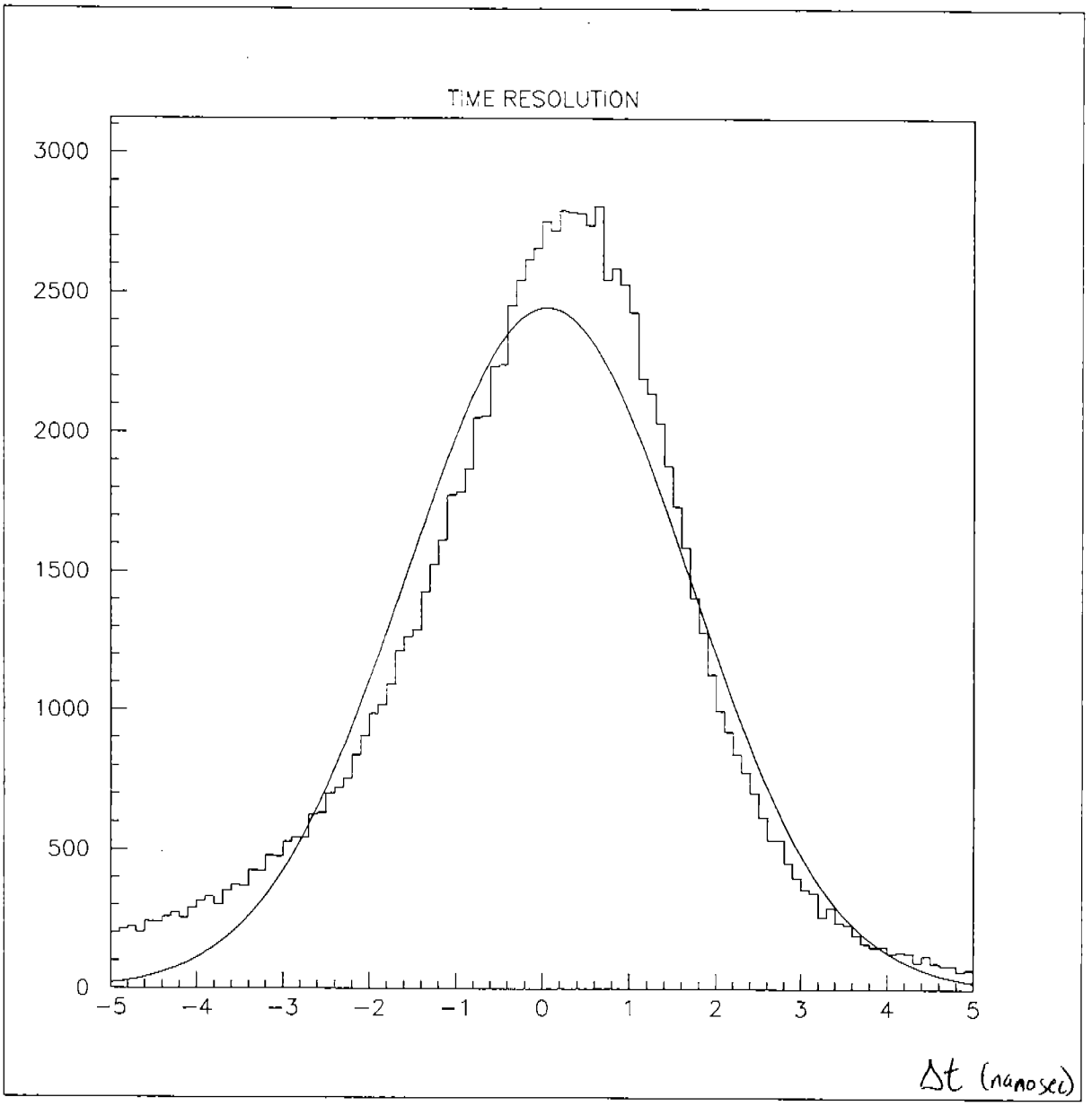

This plot is fit with a gaussian function which has a sigma of approximately 1.63 nanoseconds, which is rather poor. It is due to this poor time resolution that the completion of this study of seperating the photons from the neutrons will not be successful. Due to a lack of time, I was unable to work with this resolution problem further. Using the RF signal to improve this resolution would have allowed a better seperation between neutrons and photons. Despite this problem Figure 23 shows a plot of β versus neutron momentum.

Figure 23: β vs. Neutron Momentum

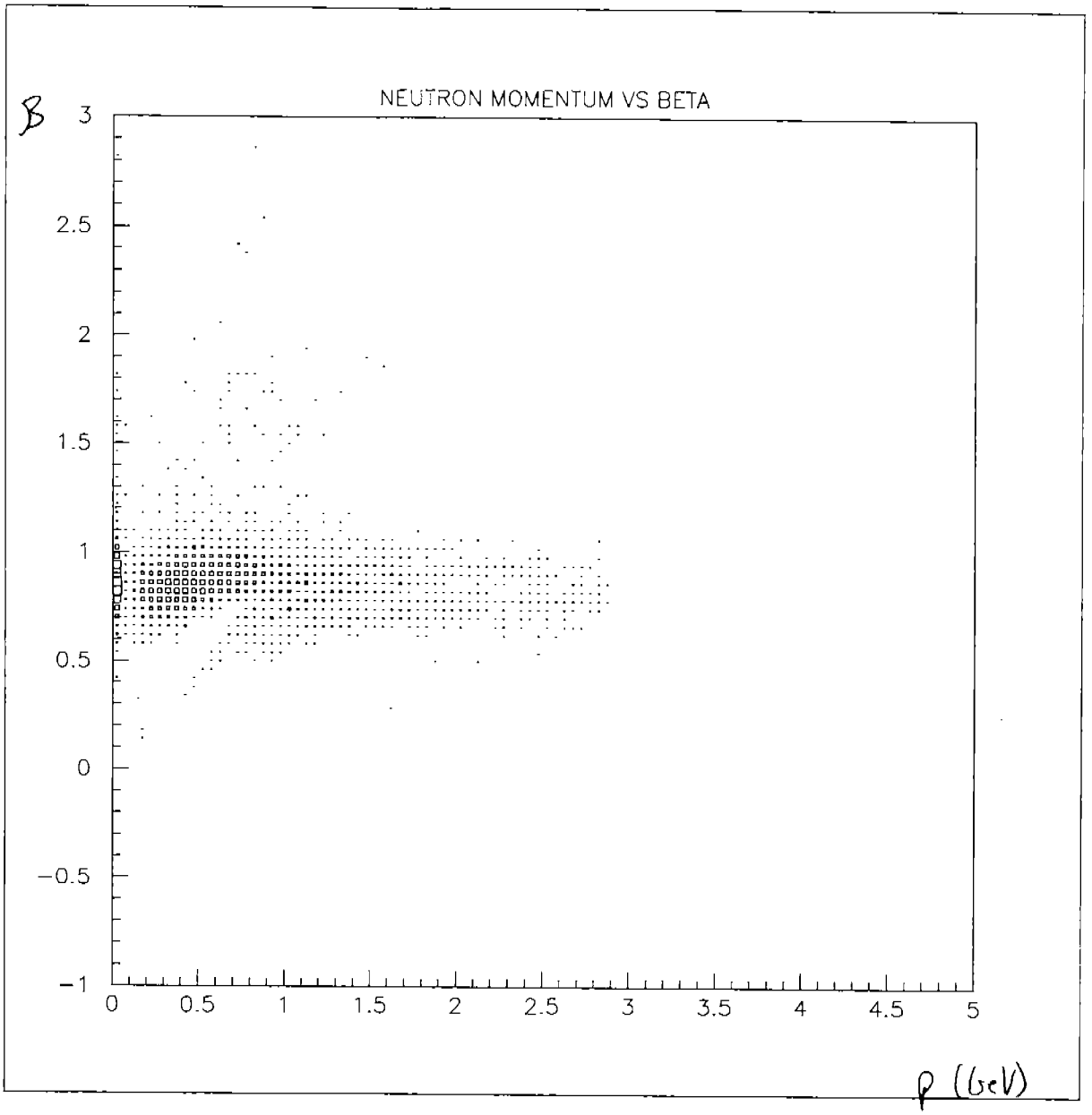

What was hoped for here was a clear separation between the neutrons and photons at low momentum. Since photons travel at the speed of light at all momentums, the photons should have been seen at a β of one and the neutrons would approach one as momentum increased. However due to the poor resolution a clear separation is not obvious, therefore, this attempt to separate the neutrons from the photons was unsuccessful. A more detailed study into the time resolution will be necessary to complete this task successfully.

Conclusions

So by using several particle identifications, fiducial cuts, a missing mass analysis, and angle cuts the final state particles were able to be identified. From this information a neutron detection efficiency as a function of neutron momentum was able to be produced, as well as, information on the angular resolution of neutron detection. In addition to this, the energy deposition of neutrons was briefly explored and an unsuccessful attempt to separate photons and neutrons was explained and its reasons for failure revealed.

Overall, the accuracy of the results on the neutron detection efficiency are good. As I mentioned before making a clearer separation between the neutrons and photons would enhance the accuracy of the results. In addition to this, it would be interesting to look at the effects the coil cuts had on the results. For example, what happens to the neutrons that hit the coils do they show up in some random sector or never make a hit at all. Also, how many of the neutrons do actually hit the coils in comparison to those that don't. For the resolution, a better error calculation would also improve those results. As it stands the resolution of the ϕ and θ angles in the drift chamber that were used to determine the predicted neutron angle were not taken into consideration. Thus, if the angular resolution in the drift chambers are poor than that would effect the neutron angular resolution. These are some of the things that would further the results of this study, however time did not permit me to look into these things myself. In any case, the results as they stand do have a high degree of accuracy and will hopefully be quite useful to many researchers.